Article:

Ardestani, MM, Moazen, M and Jin, Z (2015) Sensitivity analysis of human lower extremity joint moments due to changes in joint kinematics. Medical Engineering and Physics, 37 (2). pp. 165-174. ISSN 1350-4533

https://doi.org/10.1016/j.medengphy.2014.11.012

*Manuscript - clean copy

Original article

Sensitivity Analysis of Human Lower Extremity Joint Moments due to Changes in Joint Kinematics

Marzieh M.Ardestani[1,*], Mehran Moazen[2] and Zhongmin Jin[1, 3]

[1]State Key Laboratory for Manufacturing System Engineering, School of Mechanical Engineering, Xi'an JiaoTong University, 710049, Xi'an, Shaanxi, China

[2]Medical and Biological Engineering, School of Engineering, University of Hull, Hull, UK

[3]Institute of Medical and Biological Engineering, School of Mechanical Engineering, University of Leeds, UK

***Corresponding author: M. M. Ardestani**

Tel.: +86-029-83395122; E-mail: mostafavizadeh@yahoo.com

Word Count : Abstract to Conclusion : 4357

Abstract

Despite the widespread applications of human gait analysis, causal interactions between joint kinematics and joint moments have not been well documented. Typical gait studies are often limited to pure multi-body dynamics analysis of a few subjects which do not reveal the relative contributions of joint kinematics to joint moments.

This study presented a computational approach to evaluate the sensitivity of joint moments due to variations of joint kinematics. A large data set of probabilistic joint kinematics and associated ground reaction forces were generated based on experimental data from literature. Multi-body dynamics analysis was then used to calculate joint moments with respect to the probabilistic gait cycles. Employing the Principal Component analysis (PCA), the relative contributions of individual joint kinematics to joint moments were computed in terms of sensitivity indices (SI).

Results highlighted high sensitivity of (1) hip abduction moment due to changes in pelvis rotation (SI=0.38) and hip abduction (SI=0.4) , (2) hip flexion moment due to changes in hip flexion (SI=0.35) and knee flexion (SI=0.26), (3) hip rotation moment due to changes in pelvis obliquity (SI=0.28) and hip rotation (SI=0.4) , (4) knee adduction moment due to changes in pelvis rotation (SI=0.35) , hip abduction (SI=0.32) and knee flexion (SI=0.34), (5) knee flexion moment due to changes in pelvis rotation (SI=0.29) , hip flexion (SI= 0.28) and knee flexion (SI=0.31) , and (6) knee rotation moment due to changes in hip abduction (SI=0.32), hip flexion and knee flexion (SI=0.31).

Highlighting the “cause-and-effect” relationships between joint kinematics and the resultant joint moments provides a fundamental understanding of human gait and can lead to design and optimization of current gait rehabilitation treatments.

Keywords： Gait modification, Rehabilitation, Sensitivity analysis, Joint moments, Multi-body dynamics

1. Introduction

Human gait studies have been one of the most attractive and challenging areas of biomechanics with different applications for musculoskeletal disorder diagnosis [1-5] , therapeutic interventions[6-9] and functional evaluations of different treatments[10-13]. Multi-body dynamics (MBD) analysis has been widely used to study human gait. From a technical point of view, two different approaches of MBD analysis can be found in literature: inverse dynamics and forward dynamics. Inverse dynamics analysis has been mainly used to calculate joint moments, muscle forces and body torques from known joint kinematics [14-18] . On the other hand, forward dynamics analysis has been employed to determine the joint kinematics from known joint moments and muscle forces [19-21].

These studies however have major limitations, which prohibit a holistic understanding of human gait; first, MBD cannot provide a systematic investigation of the causal interactions between joint kinematics and the resultant joint moments. Typical gait analyses reveal the effects of joint kinematics on the joint moments and vice versa. However, the relative contributions of individual kinematics to joint kinetics cannot be well evaluated by MBD alone. Second, gait studies often do not accommodate the role of inter-patient variability. Large inter-patient variations have been reported in joint kinematics and kinetics [22, 23]. However, gait studies are often evaluated for a few numbers of subjects due to the cost and time required for experimental gait measurements.

Due to the cost of experimental data acquisition, principal component analysis (PCA) has been widely used to computationally generate a large population of probabilistic database from a small experimental data set. PCA outlines a database through its underlying principal patterns and then enlarges the database via randomizing its major patterns. For example, PCA has been used to generate large probabilistic inter-patient databases of geometry [24], elastic modulus [25] and joint kinetics [26]. Considering the inherent capability of PCA to discriminate and extract the underlying fundamental patterns of a data space, PCA has been also employed to extract and interpret the complicated interactions between highly coupled variables. For example, the relative contributions of joint alignments and loadings to joint mechanics have been investigated through PCA [27]. These two unique capabilities of PCA, enlarging a small experimental database and analyzing the causal interactions, may be hired to address the aforementioned limitations of previous MBD studies. We hypothesized that PCA can computationally produce a large probabilistic database of inter-patient joint kinematics that can be then imported to MBD to compute the corresponding joint moments. In order to perform MBD however, ground reaction forces and moments (GRF&M) , related to these probabilistic kinematics, must be first estimated . Previous studies have successfully used artificial neural network (ANN) to calculate GRF&M [34].

ANN is an efficient surrogate model with the ability to learn a nonlinear relationship [28-31]. Once a set of inputs (e.g. kinematics) and corresponding outputs (e.g. GRF&M) are presented to the network, the network learns the causal interactions between inputs and outputs. Given a new set of inputs, the trained neural network (surrogate model) can generalize the relationship to produce the associated outputs. A neural network therefore can be of significant advantage, especially when the outputs cannot be directly measured for all sets of inputs. We hypothesized that a trained ANN can be used to estimate the GRF&M related to a probabilistic database of joint kinematics that have been computationally generated through PCA. It is expected that a combination of these computational techniques can address the aforementioned limitations of the previous human gait studies.

This study developed a combined computational framework to provide a thorough quantitative insight into the essential relationships between joint kinematics and joint kinetics. Accordingly (1) a large data set of probabilistic gait cycles was created based on experimental data in literature for which (2) the qualitative contributions of individual joint kinematics to joint moments and (3) the quantitative sensitivity indices of joint moments due to kinematic variations were investigated. The aim of this study was to understand the relationships between joint kinematics and the resultant joint moments with the long term aim of optimizing current rehabilitation methods.

2. Material and methods

A published repository of experimental gait cycles was adopted for the present study (section 2.1). A large data set of probabilistic kinematics was then created from experimental gait cycles using PCA (section 2.2). Associated GRF&M were computed using ANN technique (section 2.3). MBD analysis was then employed to calculate joint moments based on the probabilistic joint kinematics and computed GRF&M (section 2.4). Once again, PCA was used to determine the contributions of joint kinematics to joint moments (section 2.5). It should be noted that PCA was used for a twofold purpose: (1) randomizing the joint kinematics and (2) extracting the interactions between kinematics and joint moments. Figure 1 shows the schematic diagram of the proposed methodology.

2.1. Experimental gait data

A subject pool consisted of four different participants (three males, one female; height: 168.3±2.6 cm; mass: 69.2±6.2kg) was adopted from a published repository (https://simtk.org/home/kneeloads). This repository included three dimensional GRF&M (Force plate, AMTI Corp., Watertown, MA, USA) , recorded with a frequency of 1000 Hz and marker trajectory data (10-camera motion capture system, Motion Analysis Corp., Santa Rosa, CA, USA) recorded at a frequency of 200 Hz for a total number of 144 gait trials. A modified Cleveland Clinic marker set was used with extra markers on the feet and trunk. These subjects walked with a variety of different patterns which provided sufficient diversity in this repository. A complete description of this data set is provided in Fregly et al (2012) [32]. A gait cycle was defined as the time interval between foot strike of one leg to the following foot strike of the same leg [33]. Subsequently, two complete gait cycles were picked up from each trial using the associated vertical GRF, leading to a total number of 288 experimental gait cycles (144 trials × two gait cycles). Joint kinematic waveforms and segmental motions were then computed using a three dimensional musculoskeletal model, implemented in MBD analysis (section 2.4). In the present study, “segmental motion” refers to “displacement” and “acceleration” of human body segments.

2.2. PCA-based statistical model

In the traditional scenario of random sampling, input parameters are perturbed independently whereas the interactions between input parameters are often ignored. Therefore, the conventional randomizing techniques (e.g., Monte Carlo, Latin hyper cube sampling, etc.) cannot be used to randomize human gait patterns since joint kinematics are highly coupled to each other and cannot be randomized separately. In other words, correspondence should be preserved between joint kinematics in order to generate a valid randomized database. To create a large database of probabilistic joint kinematics from a small experimental database, PCA was used[26]. The main idea behind this technique is to map the “inter-dependent” variables (joint kinematics) into a reduced number of corresponding “independent” variables (principal component values) that can be randomized separately. Randomized independent variables were then inversely mapped into their original inter-dependent variables. For a more detailed study of PCA technique, see [34]. Probabilistic joint kinematics were generated following the steps below:

(1) A total of 288 experimental gait cycles were arranged in a matrix X such that :

$$X = [x_1, x_2, x_3, \ldots\ldots, x_{288}] \tag{1}$$

Where x_i is a single "experimental" gait cycle:

$$x_i = [PR_x \; PR_y \; PR_z \; HA \; HF \; HR \; KF \; AF \; SE] \quad 1 \le i \le 288 \tag{2}$$

In the above equation , PRx is pelvis tilt, PRy is pelvis obliquity, PRz is pelvis rotation , HA is hip abduction/adduction, HF is hip flexion/extension , HR is hip rotation, KF is knee flexion/extension , AF is ankle flexion/extension and SE is subtalar eversion/inversion.

(2) Using PCA, a total of nine eigenvectors and the corresponding eigenvalues, associated with the above nine kinematic variables, were computed for the experimental database (X). The importance of eigenvectors was ranked with respect to the associated eigenvalues. Higher eigenvalues meant the associated eigenvectors were more essential and descriptive for the database (X) and the lower eigenvalues referred to the less-important features that might be caused by noise.

(3) The first six important eigenvectors which explained 95% of variance in X were arranged in the matrix E. The experimental data set (X) was then transformed into principal component (PC) values without significant loss of information:

$$\text{PC value} = X_{288\times 9} \times E_{9\times 6} \tag{3}$$

In other words, matrix X, consisted of nine inter-dependent kinematic variables, was transformed into a reduced number of six secondary independent variables (PC values) that can be randomized separately.

(4) For the computed PC values, row-wise mean (m) and standard deviation (d) were computed over all the 288 experimental gait cycles. Each PC value was randomly sampled from a normal distribution with a mean value of m and a standard deviation value of ±2d. Randomized PC values ($\overline{P}$) were then mapped into their original variables (joint kinematics) resulting in a probabilistic population of joint kinematics (Y) while the correspondence between coupled kinematics was preserved:

$$Y = \overline{P} \times E^{-1} \tag{4}$$

in the above equation, E^{-1} represents the inverse of matrix E.

2.3. Ground reaction force and moment computation

A number of computational techniques have been developed to calculate GRF&M only based upon kinematic waveforms [17, 35, 36]. Oh et al (2013) [35] showed feasibility of calculating ground reaction forces and moments based on joint kinematics using an artificial neural network. They proved the feasibility of using ANN-based computed GRF&M to calculate joint moments. This technique was adopted to calculate the GRF&M, related to the probabilistic joint kinematics. The methodology can be outlined as below:

(1) Using MBD software, segmental motions were calculated from probabilistic kinematics.

(2) For the single support phase, GRF&M were calculated by subtracting the gravitational acceleration from segmental acceleration regarding each human body segment (Newtonian mechanics-second law)[37].

(3) For the double support phase, a three-layer ANN with 14 inputs (displacements and accelerations of skeletal segments), three hidden neurons and six output nodes (GRF&M) was constructed (Table 1). For a

detailed description of this neural network, see [35]. This structure was trained based on two-thirds of the experimental kinematics (inputs) and the corresponding measured GRF&M (outputs) obtained from the experimental repository (section 2.1) and was validated for one-third of the remaining experimental kinematics [38]. In fact, the experimental repository was divided into three main subsets: train (70%), validation (15%) and test (15%). Once the network was trained and validated, its prediction ability was tested for those inputs that were not included in the training procedure (test subset). The trained neural network was then employed to predict the GRF&M corresponding to the double support phase of probabilistic kinematics.

(4) The cubic spline function was applied to assemble the GRF&M of single support phase (obtained from Newtonian second law) with the GRF&M of double support phase (obtained from ANN) and reconstruct the GRF&M of a complete gait cycle. All of the above computations were implemented in MATLAB (version 2009, The MathWorks, Inc., MA, USA).

2.4. Multi body dynamics analysis

A three dimensional musculoskeletal model was implemented in MBD software AnyBody Modeling System (version 6.0, AnyBody Technology, Aalborg, Denmark). This model was constructed based on the University of Twente Lower Extremity Model (TLEM). The TLEM model was a detailed cadaver-based model which has been previously validated to calculate muscle forces and joint moments[39]. The skeleton included thorax, trunk, pelvis, thigh, patella, shank and foot segments. Hip joint was modeled as a sphere joint with three degrees of freedom (DOF): flexion-extension, abduction-adduction and internal-external rotation. Knee joint was modeled as a hinge joint with only one DOF for flexion-extension and universal joint was considered for ankle-subtalar complex. The musculoskeletal model also contained 160 muscle-tendon actuators. The musculoskeletal model was scaled to the average anthropometric characteristics of four participants and was then hired in the MBD analysis at three different stages:

First, MBD analysis was employed to calculate the joint kinematic waveforms and segmental motions related to the experimental gait trials (published repository, section 2.1).

Second, MBD analysis was also used to calculate the segmental motions related to the probabilistic kinematic waveforms (section 2.2).

Third, the probabilistic kinematics (section 2.2) and the associated GRF&M (section 2.3) were imported into an inverse dynamics simulation to calculate joint moments.

2.5. PCA-based sensitivity analysis

Traditional sensitivity analysis often discards the potential dependencies between input variables and therefore is not applicable to study human gait with highly inter-dependent joint kinematics. Instead, a principal component-based technique was adopted following Fitzpatrick et al (2011) [27]. A data matrix (T) was constructed from probabilistic joint kinematics (section 2.2) and resultant joint moments (section 2.4):

$$\text{T} = [\text{joint kinematic variables},\ \text{joint kinetic variables}] \tag{5}$$

PCA was applied to calculate the eigenvectors and eigenvalues for the probabilistic gait cycles (T). Here, each eigenvector consisted of two separate parts: one part was related to the " joint kinematic variables" and the other part was related to the " joint kinetic variables". The *"kinematic*" part represented how the coupled joint kinematics varied together and the "kinetic" part explained how the resultant joint moments were changed accordingly. In other words, eigenvectors represented the relative contributions of joint kinematics to the variations of joint kinetics. Sensitivity indices were then calculated to *"rank"* the above contributions within two steps:

(1) The data matrix T was transformed into a secondary orthogonal data space of PC values:

$$\text{PC value} = T \times E_T \tag{6}$$

In the above equation, E_T is the feature matrix which contained all eigenvectors of matrix T. PC values were in fact the secondary independent variables for primary inter-dependent variables (joint kinematics and kinetics).

(2) The average PC values, over all probabilistic gait cycles, contained two separate parts associated with the "kinematic" and "kinetic" variables. The proportions of the PC values corresponding to the "joint kinematic variables" to the PC values associated with the "joint kinetic variables" were considered as the sensitivity indices (SI) of joint moments due to the joint kinematic variations.

3. Results

3.1. Generating the probabilistic gait cycles

The PCA-statistical model was randomly sampled and a total number of 500 probabilistic gait cycles were created. The sampled gait cycles were similar in pattern to the original experimental kinematics (Figure 2). Regarding each set of probabilistic joint kinematics, the trained ANN was used to estimate the GRF&M of double support phase. Figure 3 shows the average performance of the ANN. Results show that ANN could accurately predict the GRF&M of double support phase for all three subsets. All of the Pearson correlation coefficients (ρ), between network predictions (y axis) and experimental data (x axis), were above ρ=0.98. Figures (3-a) and (3-b) show that the network learned the nonlinear relationship between kinematics and

GRF&M (ρ=0.98) and Figure (3-c) implies that the network could generalize the relationship and predict the GRF&M for new kinematics which were not included in the network training (ρ=0.97). The overall patterns of estimated GRF&M were well-consistent with the experimental GRF&M (Figure 4). Computed joint moments were also similar (in terms of the overall patterns) to those joint moments which were computed based on “experimental” kinematics and “measured” GRF&M (Appendix, Figure A.1). This in turn approved the validity of the ANN-based computed GRF&M.

3.2. Relative contributions of joint kinematics

Eigenvectors are presented to demonstrate the relative contributions of individual joint kinematics to the variations of joint moments (Figure 5). For the hip joint, results indicate that the first eigenvector (the most important mode of variation) of the hip abduction moment was mainly attributed to changes in the pelvis rotation and hip abduction whilst the second eigenvector (the second important mode of variation) was highly attributed to changes in the hip joint rotation combined with knee joint flexion. PCA demonstrates the higher contributions of the pelvis rotation and hip joint abduction over the lesser contributions of other kinematics to the hip abduction moment. For hip flexion moment, first eigenvector demonstrates the higher contributions of hip flexion and knee flexion kinematics to hip flexion moment whilst the second eigenvector implies that hip flexion moment was also influenced by pelvis rotation and pelvis tilt. Similarly, hip rotation moment was mainly affected by changes in the pelvis rotation, pelvis obliquity and hip rotation.

The knee joint adduction moment was found to be sensitive to the pelvis rotation, hip abduction, and knee flexion. Eigenvectors also highlight the substantial contributions of the pelvis rotation and knee flexion (first eigenvector) to the knee flexion moment compared to the lesser contributions of the hip flexion and hip rotation (second eigenvector). Knee rotation moment was heavily influenced by hip abduction and knee flexion in the first mode of variation (first eigenvector) as well as by hip flexion in the second mode of variation (second eigenvector). For the ankle joint, results show the key relationships between knee and ankle joints flexion and ankle flexion moment. Eigenvectors also reveal that ankle joint rotation moment was highly influenced by the hip joint rotation and subtalar joint eversion.

3.3. Sensitivity indices of joint moments

Sensitivity indices (SI) of joint moments due to changes in joint kinematics are presented in Figure 6. Results highlight that hip joint abduction moment was significantly more sensitive to variations in pelvis rotation (SI=0.38) and the hip abduction (SI=0.4) than to variations in other kinematics. Hip flexion moment was noticeably sensitive to sagittal-plane kinematics including pelvis tilt (SI=0.23), hip flexion (SI=0.35), knee flexion (SI=0.26), and ankle flexion (SI=0.17). Hip rotation moment was slightly more sensitive to pelvis obliquity (SI=0.28), pelvis rotation (SI=0.22) and hip rotation (SI=0.4). Three dimensional knee joint moments (adduction, flexion and rotation components) were mainly sensitive to changes in hip and knee joints flexion ($SI \cong 0.3$). Both adduction and rotation components of the knee joint moment were highly influenced by the hip joint abduction (SI =0.32). In addition, both adduction and flexion components of the knee joint moment were sensitive to changes in pelvis rotation (for knee adduction moment: SI =0.35; for knee flexion moment: SI =0.28) but fairly insensitive to changes in pelvis tilt, pelvis obliquity and subtalar eversion. Similarly, ankle flexion moment was more sensitive to the variations in leg flexion including hip flexion (SI=0.3), knee flexion (SI=0.29) and ankle flexion (SI=0.44) while ankle rotation moment was mainly affected by the hip joint rotation (SI=0.39) and subtalar joint eversion (SI=0.29). In general, varying the kinematics of an individual joint not only changed the moment about that joint, but also could yield to substantial changes in the moments of adjacent joints. For example, hip joint abduction could noticeably affect the hip abduction moment as well as adduction and rotation components of the knee joint moment. Similarly, changes in the knee flexion led to substantial changes in three dimensional knee joint moments as well as abduction and flexion components of the hip joint moment.

4. Discussion

4.1. Relative contributions and sensitivity indices

In the conventional sensitivity analysis, a single input is perturbed while other inputs are kept constant. The individual contribution of each input to an output measure therefore can be easily perceived. This technique however cannot be employed to discriminate between different contributions of dependent inputs where all inputs are simultaneously involved to alter an output measure. For example, the overall variation in a joint moment is the result of simultaneous changes in all joint kinematics. Fitzpatrick et al (2011) [27] suggested using PCA as an alternative to interpret the "cause-and-effect" relationships between dependent inputs and outputs (section 2.5). Eigenvectors of the data space (i.e. probabilistic joint kinematics and the resultant joint moments), provided a qualitative comparison between the contributions of different kinematics (see section 3.2). For a quantitative "ranking" of the overall contributions of different joint kinematics, eigenvectors were further used to transform the inter-dependent joint kinematics and joint moments into an orthogonal data space. In the orthogonal data space, inter-dependent variables were treated as independent variables (PC values). The ratios of "joint kinematic" PC values to "joint kinetic" PC values were interpreted as sensitivity indices (see section 3.3).

4.2. Validity of the results

The fact that the patterns of probabilistic gait cycles and the computed joint moments are similar to the patterns of experimental data reassures and builds confidence in the results. Although, it cannot be guaranteed that human body replicates these patterns, our findings are well consistent with previously published clinical reports in literature. For example, our results highlight the influence of hip joint abduction and rotation kinematics on hip abduction moment which is in agreement with the study of Kraus et al (2012)[40]. PCA findings also highlight the sensitivity of knee adduction moment to changes in pelvis rotation, hip abduction/flexion/rotation, and knee flexion. Likewise, Fregly et al (2007)[41] and Barrios et al (2010)[6] demonstrated the influence of pelvis rotation, hip adduction and hip internal rotation and leg flexion on knee adduction moment. Moreover, PCA demonstrated the concurrent influence of pelvis rotation, hip flexion, hip rotation and knee flexion kinematics on knee flexion moment and knee adduction moment components (see Figure 5). Walter et al (2010)[42] and Creaby et al (2013)[43] also reported that kinematic modifications which decrease knee adduction moment may adversely increase knee flexion moment. These clinical observations can be justified according to the aforementioned multi-effect kinematics which were found to be shared between flexion and adduction components of the knee joint moment.

4.3. Applications in gait rehabilitation

Clinical biomechanics has revealed the importance of gait modification strategies in pre- and post-surgical stages [44-49]. Gait modification aims to alter joint loading distributions and decrease load on an affected limb through minor changes in the human gait pattern. Majority of the studies, concerned with the gait modification designs, are established based on conventional MBD analysis [6, 41, 50]. However, MBD alone does not provide a systematic investigation of joint kinematics that influence rehabilitation outcome.

Therefore, the synergistic joint kinematic changes, required for joint offloading, would be very challenging to determine by typical MBD.

Our findings highlighted the importance and contributions of different joint kinematics to joint moments. The most effective and ineffective joint kinematics with significant influence on joint moments were documented. Moreover, joint kinematics with simultaneous effects on adjacent joint moments were also highlighted leading to a preference or avoidance about specific kinematics to be involved in a targeted rehabilitation. These quantitative understandings therefore, can provide significant benefits in design and optimization of an objective gait retraining strategy. Considering the relative importance of kinematics, an objective rehabilitation can be designed through the most influential kinematics.

4.4. Limitations of the study

This study developed a computational framework to provide a quantitative understanding of the "cause-and-effect" interactions between joint kinematics and joint moments. To accommodate the inter-patient variability, PCA was employed to create a large probabilistic database of joint kinematics. Perhaps the main limitation of the developed framework was that the primary experimental database contained a small number of four participants. However, these subjects were quite different in anthropometric characteristics, preferred walking velocity, and shoe type. Moreover, each subject completed a variety of different walking trials ranging from normal gait to exaggerated rehabilitation patterns. Accordingly, it is expected that the present repository accommodated sufficient diversity. The second limitation was that the knee joint was modeled as a hinge joint in MBD analysis with only one DOF for flexion-extension. Nevertheless; the proposed methodology will be equally applicable for more numbers of subjects and a MBD analysis with higher DOFs.

5. Conclusion

This study provided a quantitative understanding of the interactions between joint kinematics and the resultant joint moments. A computational framework was developed to (1) generate a large database of probabilistic gait cycles, (2) assess the contributions of individual joint kinematics to the joint moments and (3) evaluate the relative sensitivity indices of joint moments due to joint kinematic variations. Results highlighted the high contributions of pelvis rotation and hip abduction to hip abduction moment, the importance of hip and knee joints flexion for hip flexion moment, and the effect of pelvis obliquity, pelvis rotation and hip rotation on hip rotation moment. Results also revealed the importance of pelvis rotation, hip abduction and knee flexion for knee adduction moment, the influence of pelvis rotation and knee flexion on knee flexion moment and the contributions of hip abduction and knee flexion to knee rotation moment. Results also showed that ankle flexion moment was highly influenced by knee and ankle joints flexion whilst ankle rotation moment was mainly influenced by hip rotation and subtalar eversion kinematics. It is expected that such quantitative insights provide potential benefits to direct the rehabilitation design procedure to optimal gait retraining programs.

Conflict of interest statement

The authors have no conflict of interests to be declared.

Acknowledgments

This work was supported by "the Fundamental Research Funds for the Central Universities", National Natural Science Foundation of China [E050702]，the program of Xi'an Jiao Tong University [grant number xjj2012108], and the program of Kaifang funding of the State Key Lab for Manufacturing Systems Engineering [grant number sklms2011001]

References

1. Böhm H, Hösl M, Schwameder H, Döderlein L. Stiff-knee Gait in Cerebral palsy: How do Patients Adapt to Uneven Ground? Gait & Posture. 2014; 39(4): 1028-33.
2. Goldberg EJ, Requejo PS, Fowler EG. Joint moment contributions to swing knee extension acceleration during gait in children with spastic hemiplegic cerebral palsy. Journal of Biomechanics. 2010; 43(5): 893-9.
3. Merory JR, Wittwer JE, Rowe CC, Webster KE. Quantitative gait analysis in patients with dementia with Lewy bodies and Alzheimer's disease. Gait & posture. 2007; 26(3): 414-9.
4. Sarkodie-Gyan T, Yu H, Alaqtash M, Abdelgawad A, Spier E, Brower R. Measurement of functional impairments in human locomotion using pattern analysis. Measurement. 2011; 44(1): 181-91.
5. Wolf SI, Braatz F, Metaxiotis D, Armbrust P, Dreher T, Döderlein L, et al. Gait analysis may help to distinguish hereditary spastic paraplegia from cerebral palsy. Gait & posture. 2011; 33(4): 556-61.
6. Barrios JA, Crossley KM, Davis IS. Gait retraining to reduce the knee adduction moment through real-time visual feedback of dynamic knee alignment. Journal of Biomechanics. 2010; 43(11): 2208-13.
7. Hunt MA, Simic M, Hinman RS, Bennell KL, Wrigley TV. Feasibility of a gait retraining strategy for reducing knee joint loading: increased trunk lean guided by real-time biofeedback. Journal of Biomechanics. 2011; 44(5): 943-7.
8. Mündermann A, Asay JL, Mündermann L, Andriacchi TP. Implications of increased medio-lateral trunk sway for ambulatory mechanics. Journal of Biomechanics. 2008; 41(1): 165-70.
9. Shull PB, Shultz R, Silder A, Dragoo JL, Besier TF, Cutkosky MR, et al. Toe-in gait reduces the first peak knee adduction moment in patients with medial compartment knee osteoarthritis. Journal of Biomechanics. 2012; 46(1): 122-8.
10. Berti L, Vannini F, Lullini G, Caravaggi P, Leardini A, Giannini S. Functional evaluation of patients treated with osteochondral allograft transplantation for post-traumatic ankle arthritis: One year follow-up. Gait & posture. 2013; 38(4): 945-50.
11. Queen RM, Appleton JS, Butler RJ, Newman ET, Kelley SS, Attarian DE, et al. Total Hip Arthroplasty Surgical Approach Does Not Alter Postoperative Gait Mechanics One Year After Surgery. PM&R. 2014;6(3):221-6
12. Queen RM, Schaeffer JF, Butler RJ, Berasi CC, Kelley SS, Attarian DE, et al. Does surgical approach during total hip arthroplasty alter gait recovery during the first year following surgery? The Journal of arthroplasty. 2013; 28(9): 1639-43.
13. Urwin SG, Kader DF, Caplan N, St Clair GA, Stewart S. Gait analysis of fixed bearing and mobile bearing total knee prostheses during walking: Do mobile bearings offer functional advantages? The Knee. 2014;21(2):391-5.
14. Forner-Cordero A, Koopman H, Van der Helm F. Inverse dynamics calculations during gait with restricted ground reaction force information from pressure insoles. Gait & posture. 2006; 23(2): 189-99.
15. Goldberg SR, Stanhope SJ. Sensitivity of joint moments to changes in walking speed and body-weight-support are interdependent and vary across joints. Journal of Biomechanics. 2013; 46(6): 1176-83.
16. Pàmies-Vilà R, Font-Llagunes JM, Cuadrado J, Alonso FJ. Analysis of different uncertainties in the inverse dynamic analysis of human gait. Mechanism and Machine Theory. 2012; 58: 153-64.
17. Ren L, Jones RK, Howard D. Whole body inverse dynamics over a complete gait cycle based only on measured kinematics. Journal of Biomechanics. 2008; 41(12): 2750-9.
18. Stagni R, Leardini A, Cappozzo A, Grazia Benedetti M, Cappello A. Effects of hip joint centre mislocation on gait analysis results. Journal of Biomechanics. 2000; 33(11): 1479-87.
19. Barrett RS, Besier TF, Lloyd DG. Individual muscle contributions to the swing phase of gait: An EMG-based forward dynamics modelling approach. Simulation Modelling Practice and Theory. 2007; 15(9): 1146-55.
20. DeWoody Y, Martin C, Schovanec L. A forward dynamic model of gait with application to stress analysis of bone. Mathematical and computer modelling. 2001; 33(1): 121-43.

21. Lim C, Jones N, Spurgeon SK, Scott J. Modelling of knee joint muscles during the swing phase of gait—a forward dynamics approach using MATLAB/Simulink. Simulation Modelling Practice and Theory. 2003; 11(2): 91-107.

22. Kutzner I, Heinlein B, Graichen F, Bender A, Rohlmann A, Halder A, et al. Loading of the knee joint during activities of daily living measured in vivo in five subjects. Journal of Biomechanics. 2010; 43(11): 2164-73.

23. Taylor WR, Heller MO, Bergmann G, Duda GN. Tibio-femoral loading during human gait and stair climbing. Journal of Orthopaedic Research. 2004; 22(3): 625-32.

24. Zhu Z, Li G. Construction of 3D human distal femoral surface models using a 3D statistical deformable model. Journal of Biomechanics. 2011; 44(13): 2362-8.

25. Bryan R, Surya Mohan P, Hopkins A, Galloway F, Taylor M, Nair PB. Statistical modelling of the whole human femur incorporating geometric and material properties. Medical engineering & physics. 2010; 32(1): 57-65.

26. Galloway F, Worsley P, Stokes M, Nair P, Taylor M. Development of a statistical model of knee kinetics for applications in pre-clinical testing. Journal of Biomechanics. 2012; 45(1): 191-5.

27. Fitzpatrick CK, Baldwin MA, Rullkoetter PJ, Laz PJ. Combined probabilistic and principal component analysis approach for multivariate sensitivity evaluation and application to implanted patellofemoral mechanics. Journal of biomechanics. 2011; 44(1): 13-21.

28. Ardestani MM, Chen Z, Wang L, Lian Q, Liu Y, He J, et al. A neural network approach for determining gait modifications to reduce the contact force in knee joint implant. Medical Engineering & Physics. 2014; 36(10): 1253-65.

29. Ardestani MM, Chen Z, Wang L, Lian Q, Liu Y, He J, et al. Feed forward artificial neural network to predict contact force at medial knee joint: Application to gait modification. Neurocomputing. 2014; 139(0): 114-29.

30. Ardestani MM, Moazen M, Jin Z. Gait modification and optimization using neural network–genetic algorithm approach: Application to knee rehabilitation. Expert Systems with Applications. 2014; 41(16): 7466-77.

31. Ardestani MM, Zhang X, Wang L, Lian Q, Liu Y, He J, et al. Human lower extremity joint moment prediction: A wavelet neural network approach. Expert Systems with Applications. 2014; 41(9): 4422-33.

32. Fregly BJ, Besier TF, Lloyd DG, Delp SL, Banks SA, Pandy MG, et al. Grand challenge competition to predict in vivo knee loads. Journal of Orthopaedic Research. 2012; 30(4): 503-13.

33. Perry J, Burnfield JM. Gait analysis: normal and pathological function: Slack; 1993.

34. Jolliffe I. Principal component analysis: Wiley Online Library; 2005.

35. Oh SE, Choi A, Mun JH. Prediction of ground reaction forces during gait based on kinematics and a neural network model. Journal of Biomechanics. 2013; 46(14): 2372-80.

36. Xiang Y, Arora JS, Abdel-Malek K. Optimization-based prediction of asymmetric human gait. Journal of Biomechanics. 2011; 44(4): 683-93.

37. Siegler S, W L. Inverse dynamics in human locomotion in three dimensional analysis of human locomotion: Wiley,New York; 1997.

38. Haykin SS, Haykin SS, Haykin SS, Haykin SS. Neural networks and learning machines: Prentice Hall New York; 2009.

39. Klein Horsman MD. The Twente lower extremity model: consistent dynamic simulation of the human locomotor apparatus: University of Twente; PhD thesis, 2007.

40. Kraus T, Švehlík M, Steinwender G, Linhart WE, Zwick EB. Gait modifications to unload the hip in children with Legg–Calve–Perthes disease. Gait & Posture. 2012; 36, Supplement 1(0): S92-S3.

41. Fregly BJ, Reinbolt JA, Rooney KL, Mitchell KH, Chmielewski TL. Design of patient-specific gait modifications for knee osteoarthritis rehabilitation. Biomedical Engineering, IEEE Transactions. 2007; 54(9): 1687-95.

42. Walter JP, D'Lima DD, Colwell CW, Fregly BJ. Decreased knee adduction moment does not guarantee decreased medial contact force during gait. Journal of Orthopaedic Research. 2010; 28(10): 1348-54.

43. Creaby MW, Hunt MA, Hinman RS, Bennell KL. Sagittal plane joint loading is related to knee flexion in osteoarthritic gait. Clinical Biomechanics. 2013; 28(8): 916-20.

44. Fransen M, (ed.) Rehabilitation after knee replacement surgery for osteoarthritis. Seminars in Arthritis and Rheumatism; 2011: Elsevier.
45. Isaac D, Falode T, Liu P, I'Anson H, Dillow K, Gill P. Accelerated rehabilitation after total knee replacement. The knee. 2005; 12(5): 346-50.
46. Klein GR, Levine HB, Hartzband MA, (eds.). Pain Management and Accelerated Rehabilitation After Total Knee Arthroplasty. Seminars in Arthroplasty; 2008: Elsevier.
47. Moffet H, Collet J-P, Shapiro SH, Paradis G, Marquis F, Roy L. Effectiveness of intensive rehabilitation on functional ability and quality of life after first total knee arthroplasty: a single-blind randomized controlled trial. Archives of physical medicine and rehabilitation. 2004; 85(4): 546-56.
48. Rahmann AE, Brauer SG, Nitz JC. A specific inpatient aquatic physiotherapy program improves strength after total hip or knee replacement surgery: a randomized controlled trial. Archives of physical medicine and rehabilitation. 2009; 90(5): 745-55.
49. Zeni Jr J, McClelland J, Snyder-Mackler L. 193 A novel rehabilitation paradigm to improve movement symmetry and maximize long-term outcomes after total knee arthroplasty. Osteoarthritis and Cartilage. 2011; 19: S96-S7.
50. Hunt M, Birmingham T, Bryant D, Jones I, Giffin J, Jenkyn T, et al. Lateral trunk lean explains variation in dynamic knee joint load in patients with medial compartment knee osteoarthritis. Osteoarthritis and Cartilage. 2008; 16(5): 591-9.

Figure

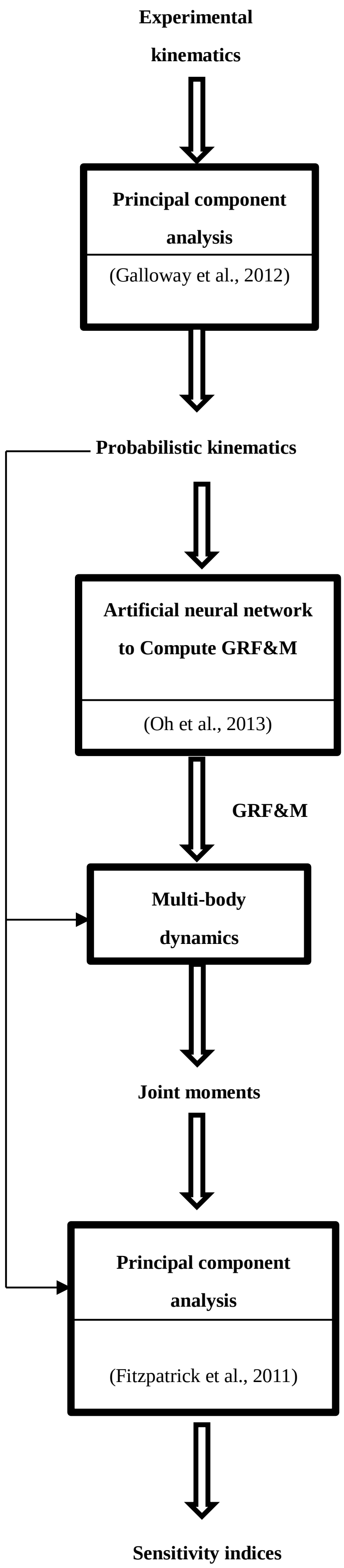

Figure 1 A schematic diagram of the proposed methodology.

Figure

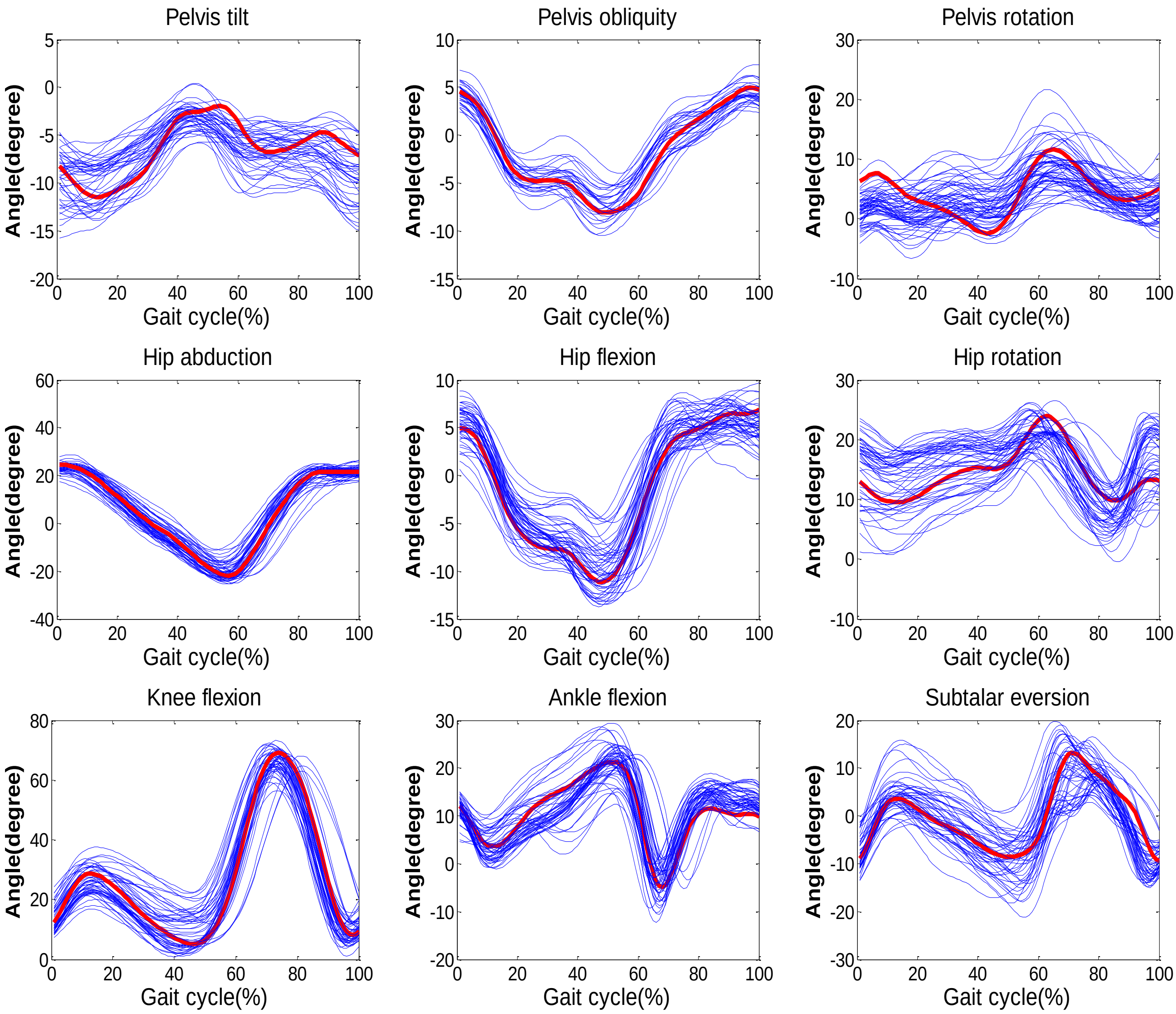

Figure 2 Probabilistic gait cycles (blue) were seen to be similar in pattern to the original experimental kinematics (red).

Figure

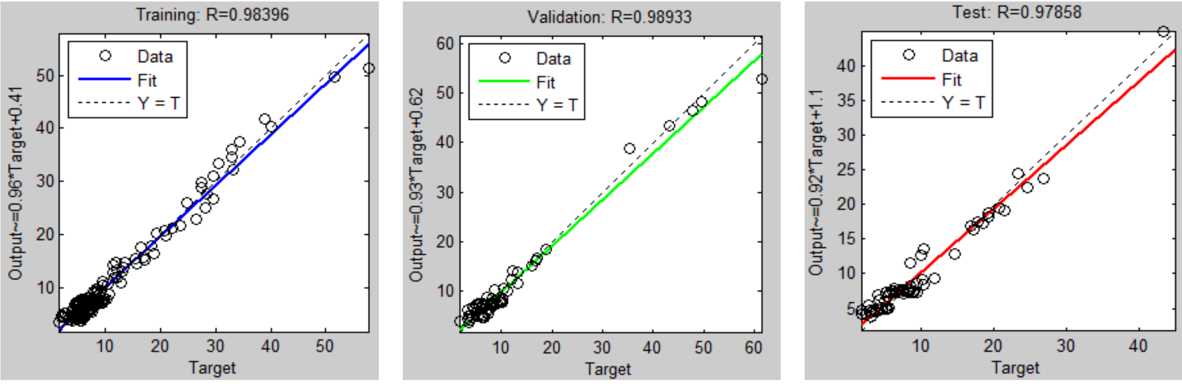

(a) (b) (c)

Figure 3 Network predictions (vertical axis) versus experimentally measured GRF&M (horizontal axis) for (a) train (b) validation and (c) test subsets.

Figure

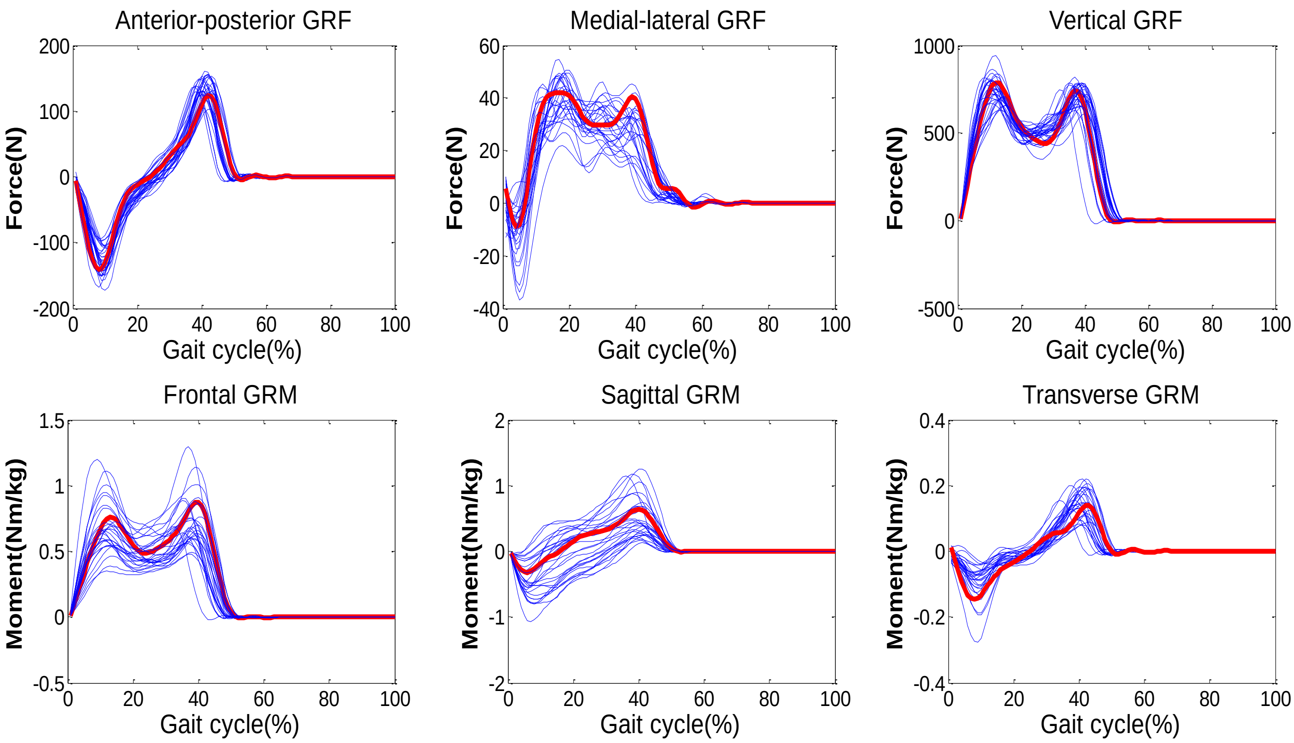

Figure 4 Predicted GRF&M (blue) were seen to match with the experimental GRF&M (red) in terms of the overall patterns.

Figure

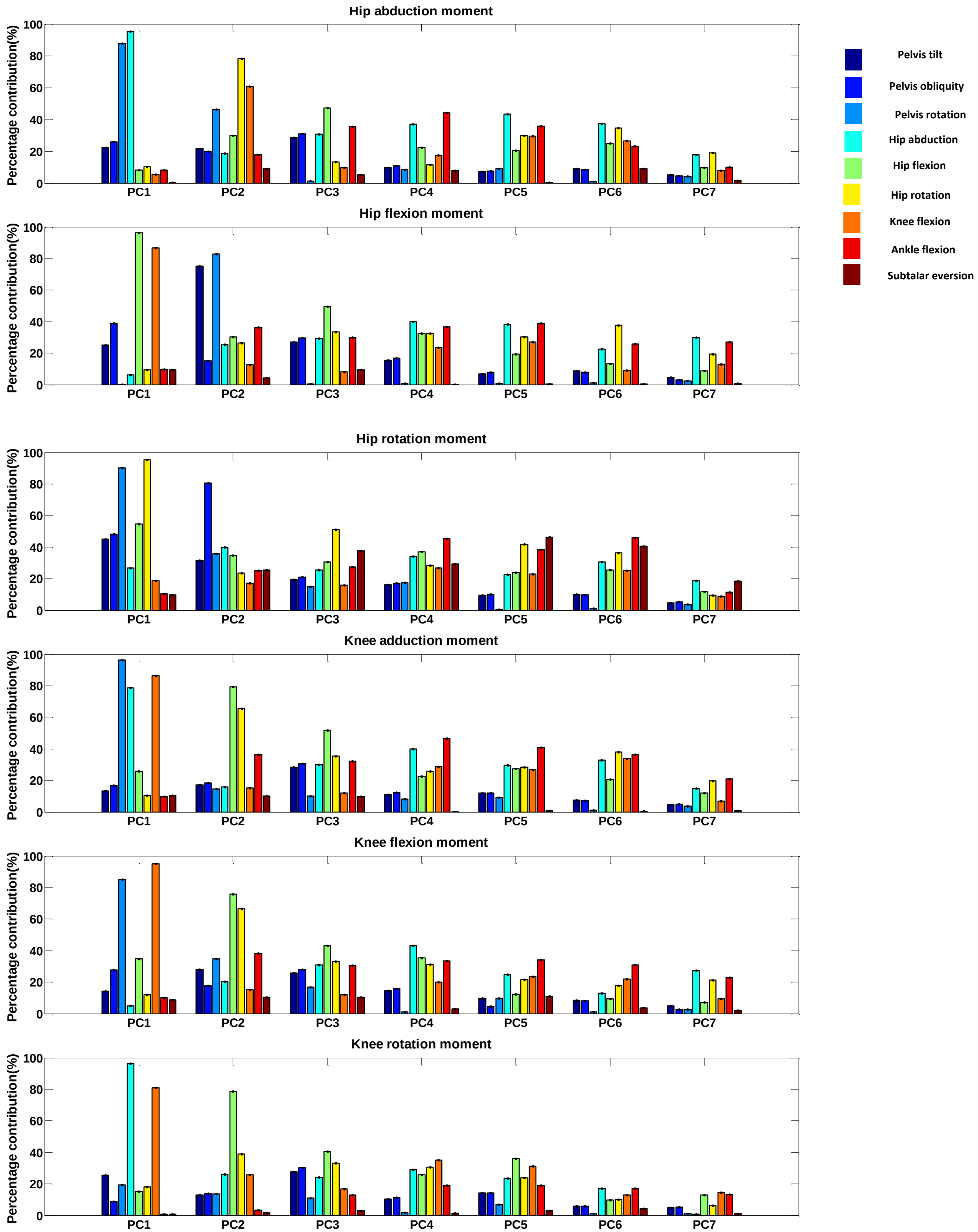

Hip abduction moment
Hip flexion moment
Hip rotation moment
Knee adduction moment
Knee flexion moment
Knee rotation moment
Percentage contribution(%)
0
20
40
60
80
100
PC1
PC2
PC3
PC4
PC5
PC6
PC7
Pelvis tilt
Pelvis obliquity
Pelvis rotation
Hip abduction
Hip flexion
Hip rotation
Knee flexion
Ankle flexion
Subtalar eversion

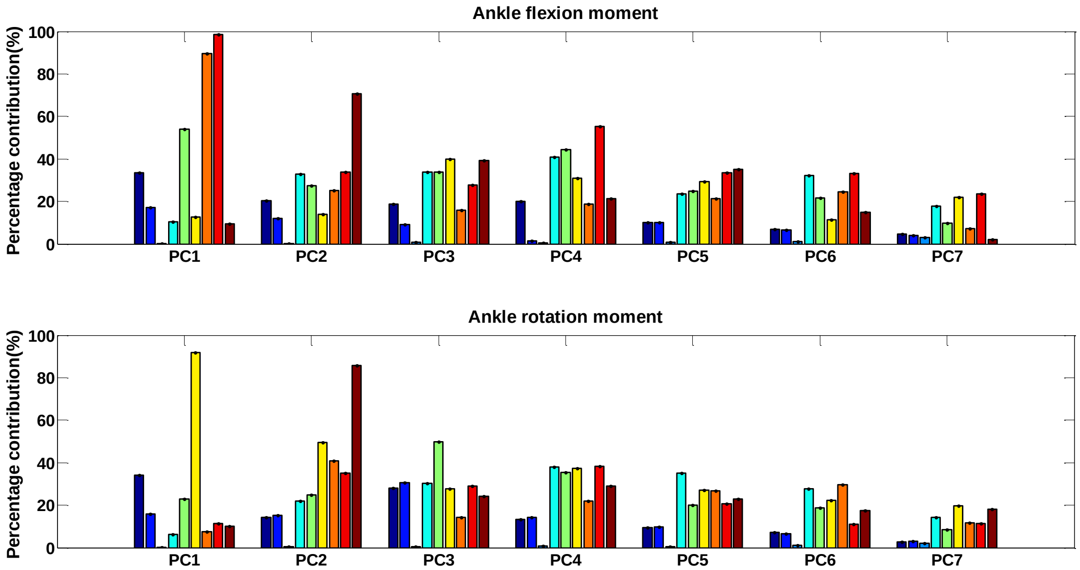

Figure 5 Eigenvectors represented the comparative contributions of individual kinematics to overall variations of the joint moments.

Figure

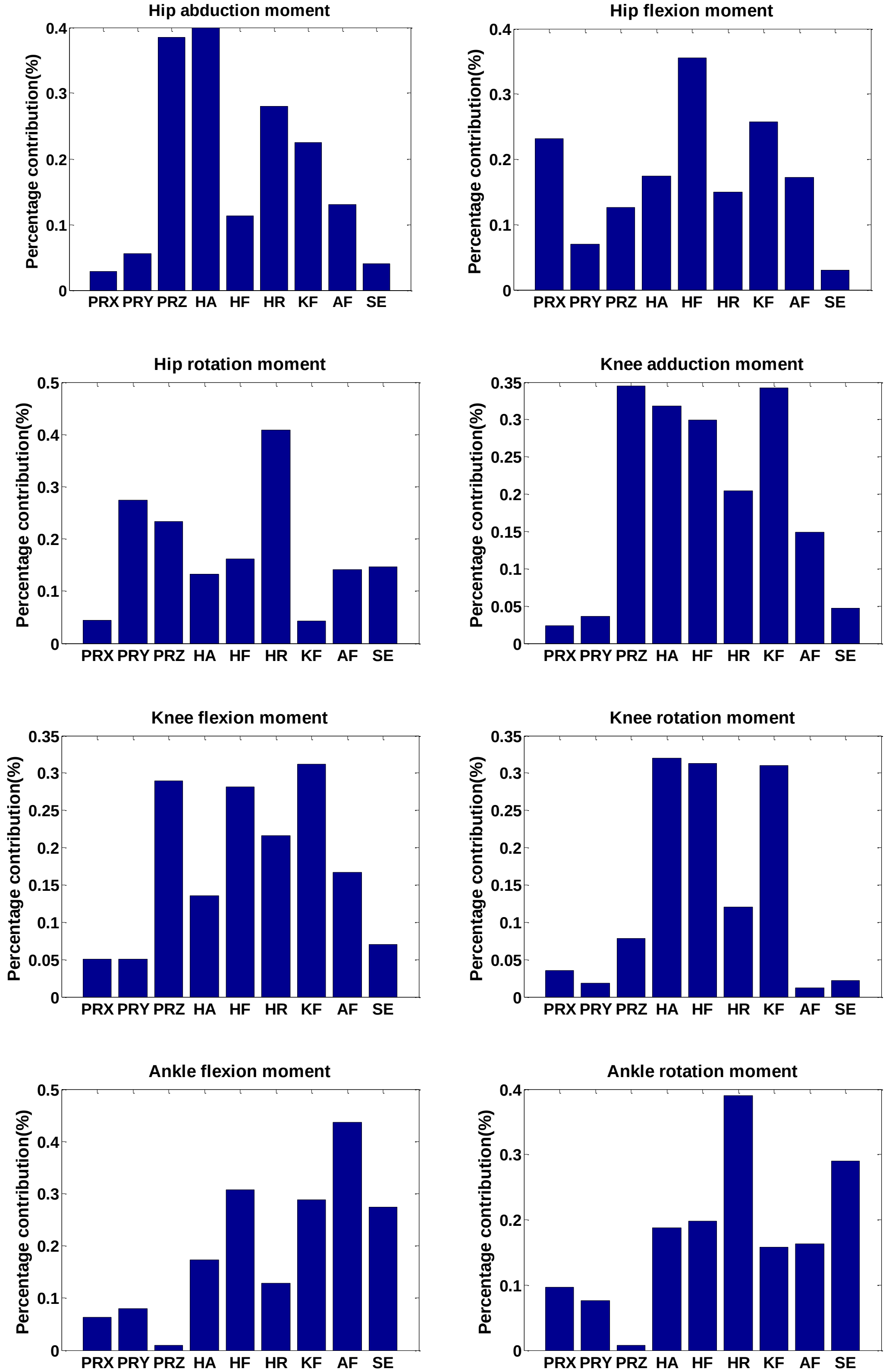

Figure 6 Quantitative sensitivity indices of joint moments due to kinematic variations (obtained from PC values).

Table

Table 1 14 input variables for artificial neural network

Input variable	Description
Displacement	Left knee joint centre in X-axis
	Left hip joint centre inY-axis
	Right ankle joint centre inZ-axis
	Left foot segment mass centre inX-axis
	Pelvis segment mass centre inX-axis
	Left thigh segment mass centre inY-axis
	Right shank segment mass centre in Z-axis
Acceleration	Thorax segment mass centre inY-axis
	Right knee joint centre inZ-axis
	Right shank segment mass centre inX-axis
	Right foot segment mass centre inY-axis
	Right thigh segment mass centre inY-axis
	Left foot segment mass centre inZ-axis
	Pelvis segment mass centre inZ-axis